Phenylketonuria: towards mechanism-based treatment

de Groot, Martijn Jonathan

Chapter 4

The absence of learning and memory deficits in C57Bl/6 Pah-enu2 PKU mice is associated with normalization of reduced pCREB to CREB ratios

Martijn J. de Groot[1-3], Vibeke M. Bruinenberg[3], Danique van Vliet[1,2], Wanda Douwenga[3], Ido P. Kema[4], Dirk-Jan Reijngoud[2,4], Francjan J. van Spronsen[1,2], Eddy A. van der Zee[3]

[1] Dept. of Metabolic Diseases, Beatrix Children's Hospital, University Medical Center Groningen, University of Groningen, Groningen, the Netherlands
[2] Center for Liver, Digestive and Metabolic Diseases, University Medical Center Groningen, University of Groningen, Groningen, the Netherlands
[3] Dept. of Molecular Neurobiology, Center for Behavior and Neurosciences, University of Groningen, Groningen, the Netherlands
[4] Dept. of Laboratory Medicine, University Medical Center Groningen, University of Groningen, Groningen, the Netherlands

Submitted to PLoS One, under revision

Abstract

In phenylketonuria (PKU), elevated brain phenylalanine concentrations and/or decreased brain concentrations of non-phenylalanine large neutral amino acids (LNAAs) likely underlie cognitive dysfunction. However, the molecular pathways and brain regions involved are only partially known. To increase pathophysiological understanding, we investigated behavioral phenotypes reflecting learning and memory, brain LNAA and neurotransmitter concentrations, and brain cAMP responsive element binding protein (CREB) phosphorylation at serine 133 (Ser-133) in C57Bl/6 Pah-enu2 PKU mice. Increased CREB Ser-133 phosphorylation is essential for learning and memory formation in several paradigms. CREB and Ser-133-phosphorylated CREB (pCREB) were studied by immunohistochemical analyses. We hypothesized that, compared to C57Bl/6 non-PKU controls, C57Bl/6 PKU mice would show a) learning and memory deficits, and b) reduced pCREB to CREB ratios in a brain-region specific manner. However, in several learning and memory paradigms, C57Bl/6 PKU mice did not show behavioral deficits. Home cage control PKU mice, which were not behaviorally tested, showed biochemical phenotypes characteristic of PKU, as well as significantly reduced pCREB to CREB ratios compared to corresponding non-PKU controls in the dentate gyrus, striatum, and somatosensory cortex. In contrast, in behaviorally tested PKU mice, pCREB to CREB ratios were comparable to those of corresponding non-PKU control mice in all brain regions of interest. Together, these data suggest that behavioral testing of C57Bl/6 PKU mice may lead to normalization of reduced pCREB to CREB ratios, thus preserving learning and memory. Further studies are indicated to characterize the processes upstream and downstream of the reduced pCREB to CREB ratios observed in home cage control PKU mice, as well as the mechanisms involved in normalizing pCREB to CREB ratios and preserving learning and memory in behaviorally tested C57Bl/6 PKU mice.

Introduction

Phenylketonuria (PKU; OMIM 261600) is an inborn error of amino acid metabolism, caused by deficiency of the hepatic enzyme phenylalanine hydroxylase (PAH; EC 1.14.16.1). PAH converts phenylalanine (Phe) into tyrosine (Tyr). PAH deficiency results in increased blood Phe concentrations and low-to-normal blood Tyr concentrations. Clinically, untreated PKU mainly manifests as a neurological disorder, with severe mental retardation as its main hallmark. PKU is diagnosed by neonatal screening and mainly treated with a Phe-restricted diet, based on a limitation of natural protein intake combined with supplementation of non-Phe amino acids. When timely diagnosed and treated, most manifestations of PKU can be prevented, in particular the severe mental retardation (1,2). However, even in patients considered to be well-treated, impairments in neuropsychological functions occur (3,4). Moreover, these patients appear to have an increased risk for psychiatric pathology (5). These outcomes in treated PKU patients indicate that current PKU treatment is not yet optimal.

An increased understanding of PKU pathophysiology could improve PKU treatment outcome. Elevated blood Phe concentrations serve as a pathophysiological starting point, as reflected by the well-established negative association between cognitive outcome in PKU and the extent of the increase in blood Phe concentration (1). Several pathophysiological mechanisms may contribute to this strong association (6,7). One particularly relevant mechanism could be reduced cerebral protein synthesis (CPS). In the field of neurobiology, the relevance of CPS for normal cognitive development has been clearly established (8,9). Clinically, this relation is supported by the finding of reduced CPS in several disorders associated with mental retardation (8-10). In PKU, reduced CPS has been reported in both animal and clinical studies (11-14). Recently, we reported that CPS rate in PKU patients shows a strong negative relationship with blood Phe concentration (15), similar to the strong negative relationship between cognitive outcome and blood Phe concentration.

One of the main molecular regulators of cognition-related CPS is cAMP responsive element-binding protein (CREB) (16-19). CREB activity is mediated by phosphorylation at serine 133 (Ser-133), which can be induced by a wide variety of stimuli and kinases (19,20). The resulting Ser-133-phosphorylated CREB (pCREB) protein is able to bind to a specific promoter sequence, leading to recruitment of additional regulatory factors and transcription of a number of genes. In turn, the newly transcribed gene products selectively increase synthesis of various proteins, and thereby orchestrate learning, memory, and cognition (16-19). Hence, in neurobiological studies investigating CREB activity in relation to protein synthesis and learning and memory, pCREB to CREB ratios are often used as a read-out

parameter (21-25).

To investigate neuronal signaling pathways and neuroanatomical substrates involved in PKU pathophysiology, the development of the Pah-enu2 PKU mouse model has been particularly valuable (26,27). In this model, PKU phenotypes result from homozygosity for the Pah-enu2 mutation, as first described in mice of the BTBR background (26). BTBR PKU mice show biochemical phenotypes in blood and brain, as well as learning and memory deficits, thus reflecting the characteristics of untreated PKU in humans (14,28-31). In 2006, the Pah-enu2 mutation was bred into wild type (WT) mice of the C57Bl/6 background to increase breeding efficiency, for the purpose of studying gene therapy (32). Another important advantage of using the C57Bl/6 background is that it has been well validated for studying learning and memory performance (33-36), and is often used in mouse models of disorders associated with mental retardation (37,38). Previous reports in C57Bl/6 Pah-enu2 mice showed that the blood and brain biochemical phenotypes of these mice are comparable to those observed in BTBR Pah-enu2 mice (39-42). However, thus far, learning and memory phenotypes of C57Bl/6 Pah-enu2 mice have not been reported.

We hypothesized that C57Bl/6 Pah-enu2 mice would show behavioral learning and memory deficits compared to C57Bl/6 non-PKU counterparts. In addition, we hypothesized that the assumed learning and memory deficits would be associated with reduced pCREB expression and/or reduced pCREB to CREB ratios. Thus, we performed a series of experiments to achieve the following two goals: (I) to characterize behavioral learning and memory phenotypes of C57Bl/6 Pah-enu2 mice and (II) to relate CREB phosphorylation data to behavioral learning and memory phenotypes of these mice.

Animals, materials and methods

Animals

Breeding and housing

A breeding colony was initiated using C57Bl/6 mice heterozygous for the p.F263S Pah-enu2 mutation, kindly provided by Prof. B. Thöny (University of Zürich, Switzerland). Mice were weaned and genotyped at 3-4 weeks of age, and subsequently housed in filter top cages in groups of 2-3 mice. Prior to behavioral testing, mice were housed individually, thus allowing for food deprivation when needed. In order to standardize housing conditions across experimental cohorts, this individual housing regime was used in all cohorts. A 12-hour light/dark cycle was maintained (lights on at 8.00 a.m.). Standard mouse chow (RMH-B 2181,

AB Diets, Woerden, the Netherlands) and water were available *ad libitum*, unless otherwise specified. Multiple mouse cohorts were tested, as shown in **Table 1**. The Animal Ethical Committee of the University of Groningen approved all experiments described below.

Table 1 Mouse cohorts and corresponding analyses.

Cohort	Composition	Gender	Age (months)	Data
1	10 WT, 13 PKU	all F	3 – 14	SA
2	4 WT, 6 HTZ, 6 PKU	all F	8 – 8.5	Brain and blood LNAAs Brain NTs
3	3 WT, 4 HTZ, 7 PKU	all F	4 – 4.5	Y-maze learning Y-maze reversal learning
4	10 WT, 10 PKU	all F	3.5 – 9.5	pCREB/CREB
5	9 WT, 8 PKU	4 M, 5 F 5 M, 3 F	14 – 16	Ten-arm radial maze Cross maze pCREB/CREB
6	5 WT, 5 PKU	3 M, 2 F 3 M, 2 F	4 – 5	Cross maze
7	16 WT, 16 PKU	8 M, 8 F 8 M, 8 F	4 – 5	NOR SOR

Characteristics of each experimental group. WT: wild type, HTZ: heterozygous, PKU: phenylketonuric. F: female, M: male. LNAAs: large neutral amino acids, NTs: neurotransmitters. SA: spontaneous alternation, NOR: novel object recognition, SOR: spatial object recognition.

Genotyping

Genotyping was performed on DNA extracted from tail tissue, by incubating tail snips with mouse-tail lysis buffer and proteinase K (100:1, volume:volume (v:v)) overnight. Next, samples were centrifuged (13.000 rpm x 10 min), supernatant was transferred to clean tubes, and isopropanol was added (1:1). Samples were centrifuged (6.000 rpm x 10 min), the supernatant was discarded, and DNA-samples were dried. Next, 200 µl Tris-HCl-EDTA-buffer (pH 8.0) was added to each sample. Samples were stored at -80 ˚C prior to genotyping. qPCR genotyping was performed on 50x diluted DNA samples. Mastermix consisted of ddH_2O, 10x PCR buffer, 50 mM $MgCl_2$, 5 mM dNTP-mix, 5 µM FAM, 5 µM Yakima Yellow, and 5 U/µl Hot Goldstar polymerase (all obtained from Eurogentec, Seraing, Belgium). 5' CCGTCCTGTTGCTGGCTTAC 3' was used as a forward primer and 3' CTAGATTCGGGTACATGTGTGGAC 5' was used as a reverse primer (both from Invitrogen, Carlsbad, USA). qPCR consisted of a 1 min cycle at 60 ˚C, a 10 min cycle at 95 ˚C, and 40 cycles of heating at 95˚C for 15 s and cooling at 60˚C for 1 min. Probe signal intensity after 25 – 30 cycles was used for genotyping. Samples were analyzed in triplicates.

Biochemical validation of the model

Amino acid concentration measurements

After inhalation anesthesia with isoflurane, blood for amino acid measurements was collected by cardiac puncture. Blood was transferred to heparinized tubes and stored on ice. Blood samples were centrifuged (12.800 rpm x 10 min), plasma was transferred to clean vials, and stored at -80 ˚C. Brain tissue was extracted after decapitation and further processed depending on follow-up analyses (see below). For brain amino acid measurements, cerebral and cerebellar tissues were separated, and both were snap frozen in liquid nitrogen. Brain tissue was stored at -80 ˚C prior to biochemical measurements. To measure blood amino acid concentrations, a solution of norleucine (72 µg/ml) and sulphosalicylic acid (75 mg/ml) was added to thawed samples (1:1, v:v). Samples were centrifuged (20.800 g x 4 min), supernatant was transferred to new vials, and LiOH was added (4:1, v:v). Next, samples were loaded into capsules, and loading buffer was added (4:1, v:v). Amino acids were separated and qualified with high-performance liquid chromatography (HPLC) followed by ninhydrin derivatization using the Biochrom 20 system (Pharmacia Biotech, Cambridge, UK). Quantification was performed according to standardized calibration techniques. Blood Trp concentrations were measured according to the serotonergic pathway protocol described below, with plasma diluted 4x in ddH_2O. Brain amino acid concentrations were measured using a procedure similar to blood concentration measurements, with the following adaptations. To obtain whole-brain homogenates, brains were grinded in liquid nitrogen. Samples were weighed and stored on dry ice. Phosphate-buffered saline (PBS, pH 7.4) was added at a 1:4 (weight:volume (wt:v)) ratio and samples were kept on ice. Next, samples were sonified for 30 s per sample at 11-12 W and centrifuged (12.800 rpm x 10 min). Supernatant was transferred to clean vials, after which the same protocol as for blood amino acid measurements was followed. Plasma concentrations were expressed as µmol/L and brain concentrations as nmol/g wet weight.

Neurotransmitter concentration measurements

For brain neurotransmitter concentration measurements, two biosynthetic pathways were assessed. First, the dopaminergic pathway, by measuring dopamine (DA) and noradrenaline (NA) concentrations. Second, the serotonergic pathway, by measuring concentrations of tryptophan (Trp), serotonin (5-HT), and 5-hydroxyindoleacetic acid (5-HIAA). Concentrations of adrenaline and 5-hydroxytryptophan were below the thresholds for reliable determination. Both pathways were assessed in brain homogenates, obtained in a similar manner as described for amino acid measurements, with the following adaptations. For the

dopaminergic pathway measurements, a homogenate buffer of glutathione (80 g/L) in 0.08 M acetic acid was used (1:20, v:v). Brain homogenates (2%, wt:v) were diluted 10x in ddH_2O, and 2,3-dihydroxybenzoic acid was added as an internal standard (10:1, v:v). Samples were analyzed by HPLC coupled to electrochemical detection. Samples were sonified and centrifuged at 4 ˚C as described above. For the serotonergic pathway measurements, 20% brain homogenates (wt:v in 0.08 M acetic acid) were added to an anti-oxidative solution of ascorbic acid (250 g/L), EDTA (104 g/L), and sodium metabisulphite (104 g/L) in ddH_2O (volume ratio 2:1:1:6). Next, 5-methyltryptophan was added as an internal standard (1:1 20% homogenate:internal standard, v:v). Samples were analyzed by HPLC coupled to fluorometric detection (Waters, Milford, MA).

Learning and memory performance

Spontaneous alternation in the Y maze

Spontaneous alternation behavior in the Y maze was used to assess spatial working memory. Performance in this paradigm involves the prefrontal cortex and the hippocampus (43,44). The Y maze consisted of three transparent plexiglas tubes (length 29 cm, diameter 4.5 cm), connected by a central sphere (diameter 8 cm), with a 120° angle between each arm. Alternation behavior was scored for 10 min, by analyzing the sequence in which mice entered different arms. Each sequence in which the three arms were subsequently entered was scored as an alternation. An entry was defined as having all paws in one arm. To prevent mice from using olfactory cues, the Y maze was cleaned with 70% ethanol between trials. Spontaneous alternation score were calculated by dividing the observed number of alternations by the number of entries minus two. Performance was analyzed by comparing spontaneous alternation scores and the number of arm entries between experimental groups.

Learning and reversal learning in the Y maze

Mice were food deprived to 85 - 90% of their *ad libitum* weight and habituated to find food in a Y maze (characteristics described above and elsewhere (45-48)). The habituation consisted of two phases. First, a 10 min free exploration of the Y maze without a food reward. Second, two sessions in which each arm was subsequently baited. In the testing phase, mice were trained to find food (0.01 – 0.05 g of standard chow) in one of two specific arms of the Y maze, which was randomized for each experimental group. To keep mice from using sensory information to locate the food reward, food was placed behind a small rim, as well as outside both the baited and non-baited arms, which contained small openings in the bottom of each arm.

The third arm served as a starting arm and was connected to a starting box. After entering an arm, the non-chosen arm was closed off with a guillotine door, manually operated by the investigator. Mice were allowed to eat the food when choosing the baited arm. Regardless of which arm was chosen, mice were kept in the starting cage after returning to it. Each animal was trained for six trials per day, with a maximum trial time of 5 min. The Y maze was cleaned with 70% ethanol between trials. For each mouse, training continued until food was obtained in at least five out of six trials for two consecutive days. Hereafter, the non-baited and baited arms were switched, to investigate reversal learning. In this way, four reversal learning series were investigated after the first learning series.

Novel object recognition and spatial object recognition tests

Figure 1A summarizes the protocols used in the novel object recognition (NOR) and spatial object recognition (SOR) tests. Both tests were performed in a square arena (50 x 50 cm). Prior to NOR and SOR testing, mice were allowed to freely explore the arena for 10 min, in order to habituate them to the testing environment. On day 1 of NOR testing, two identical objects were placed inside the arena. Mice were allowed to explore this set-up for 10 min. On NOR test day 2, one object was replaced by a novel object of a different shape. Exploration behavior was again registered during 10 min. After an interval of 5 days, the SOR test was performed in the mice previously analyzed in the NOR test. On day 1 of the SOR test, three objects with different shapes were placed inside the arena. In three 10 min trials, mice were allowed to explore the set-up. The intertrial interval was 2 min. On SOR test day 2, one of the outer objects was displaced (randomized between experimental groups), after which exploration time was again registered for 10 min. Performance in these tests was analyzed as follows. For NOR testing, the read-out parameter was the time spent on exploring the novel object compared to the non-novel object, expressed as the ratio of novel object exploration time to total exploration time of both objects. SOR test results were analyzed in three steps. First, the mean times spent exploring each object in the three sessions prior to the read-out session were calculated. Second, for each object, the difference between the exploration time in the read-out trial and the mean exploration time in the three pre-read out sessions was calculated, and expressed as a percentual difference. Third, relative exploration time differences for the non-displaced objects were averaged and compared to the relative exploration time difference for the displaced object.

Ten-arm radial maze

Ten-arm radial maze performance was primarily investigated to analyze

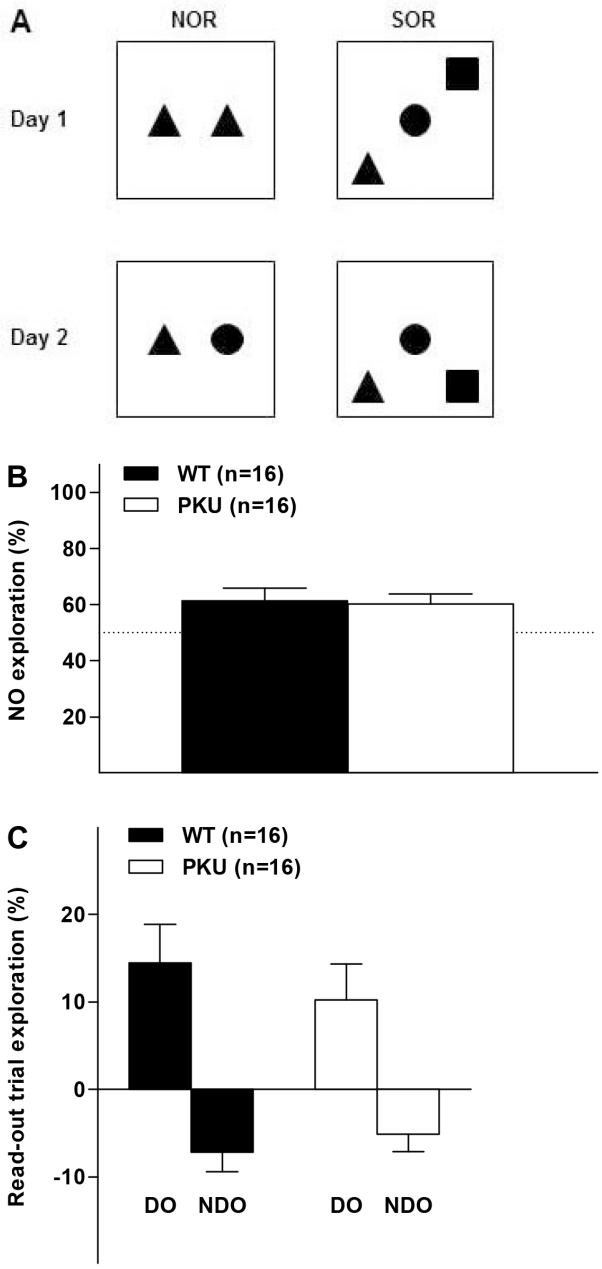

Figure 1 Set-up and performance in the NOR and SOR tests. Data were obtained in test cohort 7.
A) NOR and SOR test set-up. B) NOR test performance, expressed as novel object exploration time relative to total exploration time of both objects. The dotted line represents chance level performance. C) SOR test performance, expressed as exploration times at the read-out trial relative to the mean exploration time of three habituation trials prior to the read-out trial. WT: wild type, PKU: phenylketonuric, DO: displaced object, NDO: non-displaced objects. * $p<0.05$ for WT vs PKU.

spatial discrimination ability, a function mostly mediated by the dentate gyrus of the hippocampal formation (49-51). The custom-made ten-arm radial maze consisted of one starting arm and nine choice arms, connected by a circular arena, as shown in **Figure 2A**. Arms were 25 cm in length with a diameter of 4 cm. The central arena had a diameter of 30 cm. Prior to the testing phase, mice were food-deprived to 80-85% of their *ad libitum* bodyweight and habituated to the maze. The testing phase had the following set-up. Mice were put in a starting box connected to the starting arm. Each trial started by opening a guillotine door positioned in the starting arm. During each trial, three adjacent choice arms were opened. Of these three, the middle arm contained a food reward (0.01 – 0.05 g standard chow). All other choice arms were closed. Mice were trained to locate the food reward in the middle arm. After entering one of the three available choice arms, the two non-chosen arms were closed. An entry was defined as having all four paws in one arm. When choosing the rewarded arm, mice were allowed to retrieve the food reward. Regardless of which arm was entered, mice were maintained in the starting cage when re-entering this cage after having entered one of the choice arms. Maximum trial duration was 5 min. The position of the three choice arms relative to the starting arm (i.e. left or right as viewed from the starting arm) was randomized among experimental groups. Each mouse underwent six consecutive trials daily. During trials 1, 3, and 5, only the rewarded arm was opened. During trials 2, 4, and 6, three adjacent choice arms were opened, with only the middle arm containing a food reward. This reinforcement set-up proved to be necessary in protocol optimization experiments. To prevent mice from using sensory cues, the food reward was placed behind a small rim, and food was placed underneath small perforations in each choice arm, which could not be reached, similar to the set-up in the Y-maze learning task. Performance was scored as the percentage of correct entries. Scores were calculated per mouse before calculating the experimental group mean. Ten-arm radial maze training continued until at least one experimental group reached an average performance score of ≥ 80%.

Cross maze

After a four week wash-out phase, cross maze performance was investigated in the mice that had previously been studied in the ten-arm radial maze, using a protocol reported previously (48). The cross-maze task assesses the preference for a spatial or non-spatial strategy during food-rewarded learning. The maze consists of four arms arranged in a cross shape. Arms had a length of 27.5 cm, with a diameter of 5 cm. After food deprivation and habituation, mice were trained to locate food in one specific arm. For each mouse, the position of this food-rewarded arm relative to

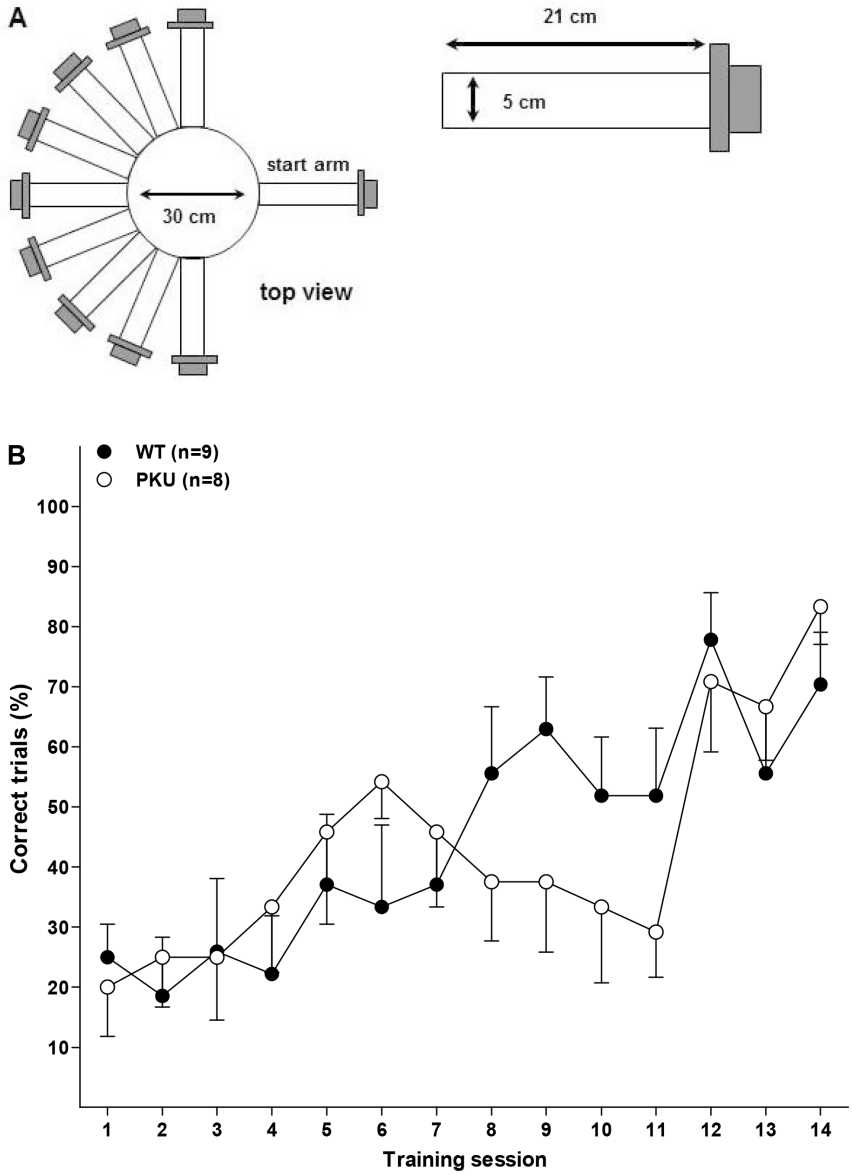

Figure 2 Set-up (A) and performance (B) in the ten-arm radial maze. WT: wild type, PKU: phenylketonuric. Results are shown as mean with SEM. Data were obtained in test cohort 5.

the starting arm (i.e. left or right) was the same as in the ten-arm radial maze. During the testing phase, the starting arm and two choice arms were opened. Mice were able to enter the starting arm from a starting box. The arm opposing the start arm was closed. Six consecutive trials were performed daily, with a maximum trial duration of 5 min. Performance was scored as the percentage of correct trials per day. Based

on data previously obtained in our group (48), cross-maze training continued for four days. In order to prevent overtraining, which could bias probe trial results, mice with at least 5 out of 6 correct trials on training day two were exposed to three trials (rather than six trials) on subsequent training days. Following cross-maze training, a probe trial was performed. In this trial, the arm opposing the starting arm became the new starting arm, while the original starting arm was closed off. Performance in the probe trial was interpreted as follows. Mice using a spatial strategy will locate the food reward based on a spatial mind map, and will thus be able to retrieve the food reward during the probe trial. Mice using a non-spatial strategy will have learned to take a specific turn when approaching the cross point, and thus be unable to retrieve the food reward during the probe trial. These principles are discussed in more detail elsewhere (52,53). Prior to starting the probe trial, mice were kept in the starting box for 2 min, to allow spatial orientation for mice using a spatial strategy. During the probe trial, both arms were baited with food, to reduce a possible influence of probe trial performance on immunohistochemical markers. Mice were euthanized 100 min after the probe trial to obtain brain tissue for immunohistochemical analyses.

CREB and pCREB immunohistochemistry

Mice were anesthetized with O_2/CO_2 and transcardially perfused with a NaCl 0.9%/heparin 0.5% solution, followed by perfusion with 4% paraformaldehyde (PFA) and ddH_2O. Brains were removed and stored in 4% PFA at room temperature for postfixation during 24 hrs. Hereafter, the PFA solution was replaced with a 0.01 M PBS solution (pH 7.4) and stored at 4 ˚C for 24 hrs. In order to dehydrate the brain tissue, the PBS solution was changed for a 30% sucrose solution (in ddH_2O), to which brains were exposed for 12 - 24 hrs. Next, brains were rinsed with 0.01 M PBS, frozen with liquid nitrogen, and stored at –80 ˚C before further processing. Brain sectioning was performed using a Leica CM3050 cryostat (Leica Microsystems, Rijswijk, the Netherlands) with a section diameter of 20 µm. Sections were collected according to the following Bregma coordinates: +2.80 to +1.10 mm (prefrontal cortex), +1.10 to -0.94 mm (striatum), -0.94 to -2.46 mm (somatosensory cortex and hippocampal formation). Free-floating sections were stored in 0.01 M PBS (pH 7.4) with 0.01% sodium azide at 4 ˚C prior to staining. The staining protocol consisted of the following steps. First, sections were rinsed with 0.01 M PBS. To quench endogenous peroxidase activity, sections were pretreated with 0.3% H_2O_2 for 30 min at room temperature. Next, sections were again rinsed with 0.01 M PBS. Sections were incubated with primary antibody in 0.01 M PBS, which additionally contained 2% BSA and 0.1% Triton X-100, at 4 ˚C overnight to 72 hrs (depending on the antibody of interest). The primary antibodies investigated were CREB (ab32515, 1:2000;

Abcam, Cambridge, UK) and pCREB (Ser-133, 06-519, 1:1000; Millipore, Temecula, USA). After primary antibody incubation, sections were rinsed and incubated with a biotinylated goat-anti-rabbit secondary antibody (1:500; Jackson Laboratories, Bar Harbor, USA) in 0.01 M PBS with 0.1% Triton X-100 for both primary antibodies for 2 h at room temperature. After rinsing with 0.01 M PBS, sections were incubated with a streptavidin-biotin complex (1:500, Vector Laboratories, Burlingame, USA) for 2 hrs at room temperature. Staining was performed with 3,3'-diaminobenzidine (DAB, 0.35 mg/ml; SigmaFast, Amsterdam, the Netherlands) and initiated by adding 100 µl 0.1% H_2O_2 to 3 ml solution. The staining reaction was stopped by changing the DAB solution for 0.01 M PBS. The next day, sections were mounted from a 1% gelatin solution onto Superfrost™ microscope slides (Thermo Fisher Scientific, Waltham, USA), passed through an ethanol/xylol series, and air-dried for 24 hrs. Finally, sections were covered with a glass cover plate. Immunohistochemical analyses were performed using a Quantimet image analyzer (Leica Camera AG, Solms, Germany). **Table 2** shows the immunohistochemical measurement characteristics for CREB and pCREB. For CREB and pCREB immunoreactivity in the striatum, analyses were made in a dorsomedial, dorsolateral, and ventromedial measurement area, using a sampling template of 450 µm^2. For CREB and pCREB immunoreactivity in the cortex, the measurement area was positioned at the somatosensory cortex overlying CA2, and included cortical layers I – VI. For all brain regions of interest, the corrected optical density (i.e. the optical density in a region of interest minus the optical density in a background region) for CREB and pCREB was determined. In each animal, three sections were used to calculate mean values for CREB corrected optical density (OD), pCREB corrected OD, and corresponding pCREB/CREB ratios. Next, these data were compared between WT and PKU mice. pCREB to CREB ratios served as the primary outcome parameter.

Table 2 Immunohistochemical measurement characteristics for CREB and pCREB.

Region	Expression pattern	Background
DGi	neuronal nuclei granular layer	CA3 stratum oriens
DGo	neuronal nuclei granular layer	CA3 stratum oriens
CA1	neuronal nuclei pyramidal layer	CA1 stratum oriens
CA3	neuronal nuclei pyramidal layer	CA3 stratum oriens
STR	neuronal nuclei	corpus callosum
CORT	neuronal nuclei layers I – VI	CA1 stratum oriens
PFC	neuronal nuclei	prelimbic and orbital cortex

DGi: inner layer of the dentate gyrus; DGo: outer layer of the dentate gyrus; CA: cornu ammonis; STR: striatum, measured in a dorsomedial, dorsolateral, and ventromedial area; CORT: somatosensory cortex, measured in cortical tissue overlying CA2; PFC: prefrontal cortex.

Statistical analyses

Normality of distributions and homogeneity of variances were tested using the Shapiro-Wilk and Levene's tests, respectively. In case of normal distribution with similar variance, experimental groups were compared using Student's t-test and ANOVA tests with Bonferroni post-hoc testing. Otherwise, the Mann-Whitney U test and Kruskal-Wallis tests were used. Specific univariate and multivariate ANOVA tests were performed as indicated. Fisher's exact test was used to analyze the data on choice-making behavior in the 10-arm radial maze and performance at the cross-maze probe trial. A p-value <0.05 was considered to be statistically significant.

Results

Biochemical validation of the model

Amino acid and neurotransmitter concentration measurements

Blood and brain amino acid concentrations did not differ significantly between WT and heterozygous (HTZ) mice. Therefore, data from these non-PKU control mice were pooled. **Table 3** shows blood and brain amino acid concentrations, as well as brain concentrations of neurotransmitters and associated metabolites in PKU mice and non-PKU controls. PKU mice showed increased blood Phe concentrations and decreased blood Tyr concentrations compared to non-PKU controls ($p<0.001$ for both). Blood concentrations of the additional LNAAs did not differ significantly between PKU mice and non-PKU controls. Brain LNAA concentration measurements showed increased brain Phe concentrations in PKU mice compared to non-PKU mice ($p<0.001$). These elevated brain Phe concentrations were paralleled by reduced brain concentrations of several non-Phe LNAAs, which were decreased by 20-40% of non-PKU control values. Specifically, these reductions concerned valine, methionine, tyrosine, and tryptophan ($p=0.015$, $p=0.032$, $p=0.023$, and $p=0.001$, respectively), with a statistical trend for threonine ($p=0.063$).

Brain neurotransmitter marker concentrations were determined for the dopaminergic and serotonergic pathways. Brain dopamine and brain noradrenaline concentrations were decreased in PKU mice, by ~30% and ~45% compared to non-PKU controls, respectively ($p<0.001$ for both). Brain serotonin and 5-HIAA concentrations were decreased in PKU mice, both by ~60% compared to WT controls ($p<0.001$ for both).

Learning and memory performance

Spontaneous alternation in the Y maze

Figure 3A shows spontaneous alternation performance in the Y maze.

Spontaneous alternation scores did not differ between WT and PKU mice (WT 63 ± 13% vs PKU 65 ± 10%, p=0.716). The number of arm entries of WT and PKU mice was comparable (WT 29 ± 9 vs PKU 28 ± 9, p=0.511).

Table 3 Blood LNAA concentrations (μmol/L), brain LNAA concentrations (nmol/g wet weight) and brain neurotransmitter marker concentrations (nmol/g wet weight) per experimental group.

	Non-PKU control (n=10)	PKU (n=6)	p
Blood LNAAs			
Threonine	234 ± 67	196 ± 51	0.259
Valine	327 ± 50	336 ± 60	0.765
Methionine	58 ± 14	52 ± 11	0.387
Isoleucine	127 ± 15	122 ± 20	0.575
Leucine	232 ± 33	214 ± 32	0.292
Tyrosine	99 ± 24	49 ± 6*	<0.001
Histidine	101 ± 22	90 ± 16	0.348
Tryptophan	87 ± 15	75 ± 15	0.143
Phenylalanine	122 ± 17	1954 ± 380*	<0.001
Brain LNAAs			
Threonine	392 ± 75	320 ± 56	0.063
Valine	124 ± 20	91 ± 28	0.015
Methionine	32 ± 8	23 ± 5	0.032
Isoleucine	75 ± 20	62 ± 21	0.236
Leucine	173 ± 49	141 ± 50	0.234
Tyrosine	112 ± 35	71 ± 21	0.023
Histidine	137 ± 39	160 ± 25	0.226
Tryptophan	46 ± 5	35 ± 1	0.001
Phenylalanine	130 ± 42	685 ± 53	<0.001
Brain NT markers			
Dopamine	6.970 ± 0.450	5.059 ± 0.332	<0.001
Noradrenaline	2.754 ± 0.136	1.560 ± 0.088	<0.001
Serotonin	2.148 ± 0.299	0.914 ± 0.145	<0.001
5-HIAA	3.239 ± 0.163	1.292 ± 0.193	<0.001

Data were obtained in test cohort 2. Results are shown as mean ± standard deviation. PKU: phenylketonuric, LNAA: large neutral amino acid, NT: neurotransmitter.

Learning and reversal learning in the Y maze

Learning and reversal learning results in the Y maze are shown in **Figures 3B-D**. Both PKU mice and non-PKU mice mastered the paradigms. Data from WT and HTZ mice were pooled, as in each testing phase, performance scores for these non-PKU control mice were not significantly different. **Figures 3B and 3C** show

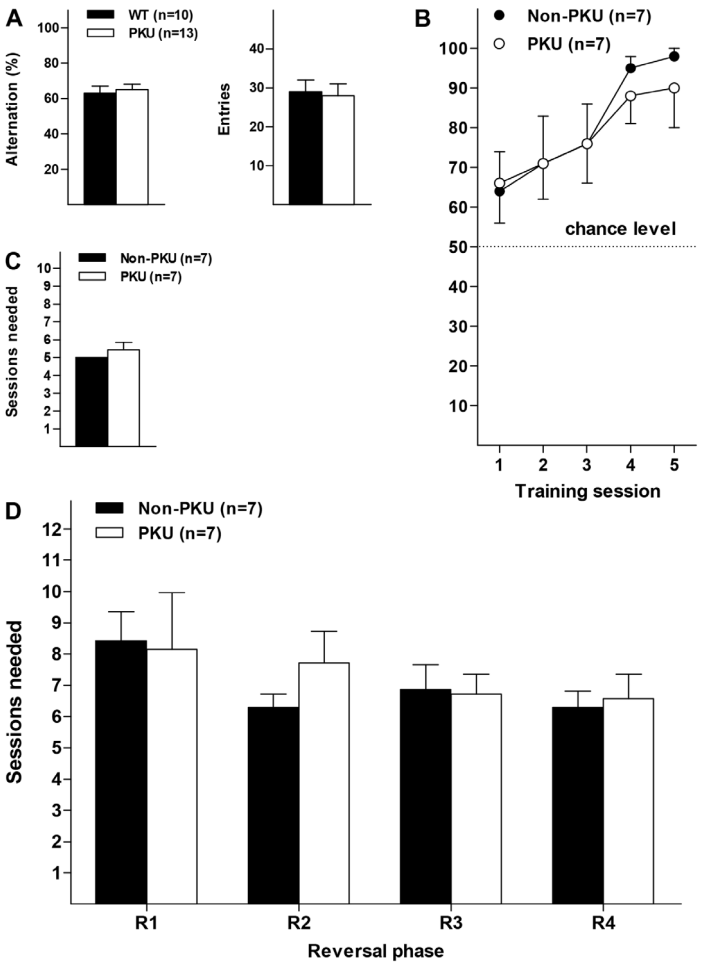

Figure 3 Performance in Y maze-related paradigms. A) Spontaneous alternation score and number of entries in the Y maze. B) Performance in the learning phase of Y-maze experiments. C) Number of sessions needed to pass the learning criterion in the learning phase. D) Reversal training performance in the Y maze. Results are given as mean ± SEM. WT: wild type, PKU: phenylketonuric. These data were obtained in test cohorts 1 and 3.

the performance of PKU mice and non-PKU controls in the learning phase. Mixed-design ANOVA showed a main effect for training session ($F=6.043$, $p=0.007$), but not for experimental group ($F=0.082$, $p=0.780$). There was no interaction effect between training session and experimental group ($F=0.181$, $p=0.840$). **Figure 3D** shows the performance of PKU mice and non-PKU controls in the reversal phases. Reversal phase data were analyzed by mixed-design ANOVA, with reversal phase as within-subjects factor and experimental group as between-subjects factor. Reversal phase

did not have a main effect on the number of sessions needed to pass the learning criterion (F=1.431, p=0.250). Both the main effect for experimental group and the interaction effect between reversal phase and experimental group were non-significant (F=0.227, p=0.642 and F=0.330, p=0.804, respectively).

Novel object recognition and spatial object recognition tests

Figures 1B and 1C show NOR and SOR test performance. For both tests, data were analyzed by two-way independent ANOVA, with genotype and gender as factors. In the NOR test, both WT and PKU mice performed above chance level (p=0.019 and p=0.008, respectively). Two-way ANOVA showed no main effect of genotype (F=0.040, p=0.843), no main effect of gender (F=2.372, p=0.135), and no interaction effect between genotype and gender (F=0.222, p=0.641). In the SOR test, both WT and PKU mice were able to recognize the displaced object, performing above chance level (p=0.005 and p=0.024, respectively). Two-way ANOVA showed no main effect of genotype (F=0.544, p=0.467), no main effect of gender (F=2.714, p=0.111), and no interaction effect between genotype and gender (F=2.861, p=0.102).

Ten-arm radial maze

Ten-arm radial maze performance is shown in **Figure 2B**. All mice gradually learned to distinguish the baited arm from the non-baited arms. Mixed-design ANOVA showed a main effect of training session (F=6.212, p<0.001). Genotype did not have a main effect (F=0.018, p=0.894). There was no interaction effect between training session and genotype (F=1.320, p=0.210).

Cross maze

Figures 4A and 4B show cross-maze performance during the training sessions and probe trial in the mice previously tested in the ten-arm radial maze. Mixed-design ANOVA showed a main effect of training session on cross-maze performance (F=10.695, p=0.001), without a main effect of genotype (F=1.051, p=0.332). There was no interaction effect between training session and genotype (F=0.800, p=0.429). In the probe trial, both WT and PKU mice showed a preference for making the same turn as during the training sessions, consistent with favoring a non-spatial strategy over a spatial strategy. Probe trial results did not differ between WT and PKU mice (p=1.000). To investigate whether a carryover effect could have influenced these data, cross-maze performance was additionally assessed in mice without previous exposure to behavioral testing. **Figures 4C and 4D** show cross-maze performance of these mice. The results of mice without previous behavioral testing were similar

to those of mice previously tested in the ten-arm radial maze, showing comparable training performance curves in both genotype groups, with main effect of training session as the only significant effect ($F=9.959$, $p<0.001$). Again, in the probe trial, a strong preference for a non-spatial strategy was observed in both genotype groups. This preference did not differ between genotype groups ($p=1.000$).

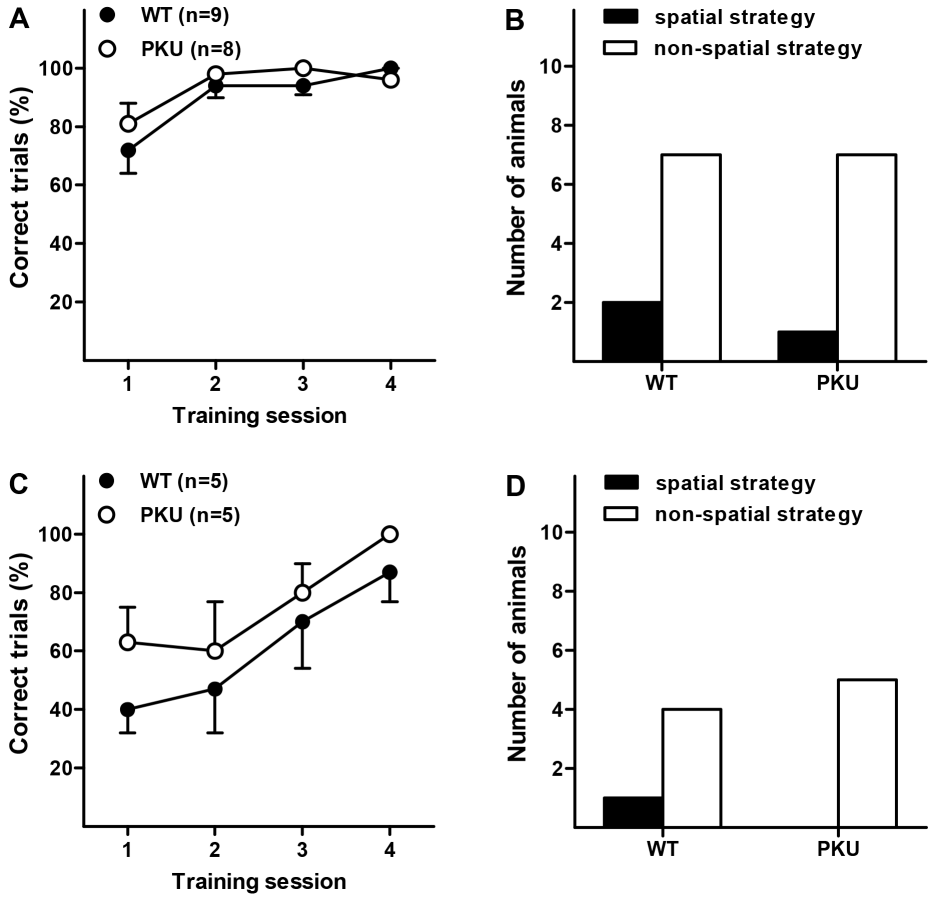

Figure 4 Cross-maze performance during training and in the probe trial in mice previously tested in the ten-arm radial maze (A,B; test cohort 5) and in mice without previous behavioral testing (C,D; test cohort 6). WT: wild type, PKU: phenylketonuric. Results are shown as mean ± SEM.

CREB and pCREB immunohistochemistry

CREB and pCREB expression in home cage control mice

Consistent with previous reports (19,48,54) and known physiological functions, both CREB and pCREB were expressed in neuronal nuclei throughout the brain. We focused on CREB and pCREB staining in the dentate gyrus, CA1, CA3, striatum, somatosensory cortex, and prefrontal cortex. CREB and pCREB expression patterns

were comparable for WT and PKU mice. Since CREB and pCREB staining in the striatum did not differ significantly between subregions (regardless of genotype), striatal subregion data were pooled for each genotype. Prior to comparing mean pCREB to CREB ratios between WT and PKU mice, CREB and pCREB corrected OD values were compared between these genotype groups. **Table 4** and **Figure 5A** show CREB corrected OD values, pCREB corrected OD values, and corresponding pCREB to CREB ratios in home cage control WT and PKU mice (which were not behaviorally tested).

Mean CREB corrected OD values and mean pCREB corrected OD values did not differ significantly between PKU and WT mice in the brain regions of interest. However, mean pCREB/CREB corrected OD ratios in PKU mice were significantly lower than WT values in the dentate gyrus, the striatum, and the somatosensory cortex. In these brain regions, mean ratios of PKU mice were reduced by approximately 5% to 20% compared to mean WT ratios. In the CA1 and CA3 regions of the hippocampal formation, as well as in the prefrontal cortex, mean pCREB/CREB corrected OD ratios did not differ significantly between WT and PKU mice. When interpreting immunohistochemical pCREB/CREB ratios, it should be noted that these ratios may be >1, as antibody-specific background OD values were used to calculated corrected OD values, and signal intensities for pCREB and CREB may differ at similar amounts of the protein of interest, due to different binding affinities of the anti-pCREB and anti-CREB antibodies.

CREB and pCREB expression in behaviorally tested mice

The cellular distribution patterns of CREB and pCREB in behaviorally tested mice were comparable to the corresponding patterns in home cage control mice. As in home cage control mice, CREB and pCREB staining in the striatum did not differ significantly between subregions in behaviorally tested mice (regardless of genotype). Therefore, striatal subregion data of behaviorally tested mice were pooled for each genotype. **Table 4** and **Figure 5B** show CREB corrected OD values, pCREB corrected OD values, and corresponding pCREB to CREB ratios in behaviorally tested WT and PKU mice. Mean CREB corrected OD values and mean pCREB corrected OD values in behaviorally tested WT and PKU mice did not differ significantly for the dentate gyrus, CA1, CA3, striatum, somatosensory cortex, and prefrontal cortex. Contrary to the findings in home cage control PKU mice, mean pCREB to CREB corrected OD ratios in behaviorally tested PKU mice were not significantly different from corresponding WT values in any brain region.

Table 4 Corrected OD values for CREB and pCREB with associated pCREB/CREB ratios per experimental group.

	Home cage control			Behaviorally tested		
	WT (n=10)	**PKU (n=10)**	**Δ**	**WT (n=9)**	**PKU (n=8)**	**Δ**
CREB						
DGi	0.27 ± 0.08	0.31 ± 0.07	+15%	0.27 ± 0.08	0.31 ± 0.07	+15%
DGo	0.28 ± 0.08	0.32 ± 0.09	+14%	0.51 ± 0.05	0.54 ± 0.05	+6%
CA1	0.47 ± 0.06	0.46 ± 0.09	-2%	0.39 ± 0.04	0.41 ± 0.03	+5%
CA3	0.14 ± 0.03	0.15 ± 0.03	+7%	0.18 ± 0.02	0.20 ± 0.05	+11%
STR	0.60 ± 0.03	0.63 ± 0.03	+5%	0.56 ± 0.03	0.56 ± 0.02	0%
CORT	0.08 ± 0.01	0.09 ± 0.02	+13%	0.06 ± 0.01	0.07 ± 0.01	+17%
PFC	0.62 ± 0.05	0.62 ± 0.05	0%	0.58 ± 0.03	0.60 ± 0.01	+3%
pCREB						
DGi	0.32 ± 0.07	0.31 ± 0.07	-3%	0.37 ± 0.08	0.37 ± 0.09	0%
DGo	0.28 ± 0.07	0.27 ± 0.06	-4%	0.34 ± 0.07	0.34 ± 0.07	0%
CA1	0.18 ± 0.07	0.18 ± 0.05	0%	0.21 ± 0.04	0.22 ± 0.06	+5%
CA3	0.12 ± 0.04	0.13 ± 0.03	+8%	0.10 ± 0.03	0.11 ± 0.02	+10%
STR	0.47 ± 0.02	0.46 ± 0.02	-2%	0.48 ± 0.06	0.47 ± 0.03	-2%
CORT	0.16 ± 0.01	0.15 ± 0.02	-6%	0.07 ± 0.02	0.08 ± 0.02	+14%
PFC	0.36 ± 0.04	0.35 ± 0.03	-3%	0.44 ± 0.02	0.44 ± 0.03	0%
pCREB/CREB						
DGi	1.23 ± 0.21	1.03 ± 0.14*	-16%	0.69 ± 0.12	0.70 ± 0.13	+1%
DGo	1.04 ± 0.15	0.88 ± 0.11*	-15%	0.66 ± 0.10	0.62 ± 0.08	-6%
CA1	0.39 ± 0.14	0.40 ± 0.11	+3%	0.53 ± 0.08	0.52 ± 0.11	-2%
CA3	0.94 ± 0.26	0.93 ± 0.18	-1%	0.54 ± 0.12	0.57 ± 0.10	+6%
STR	0.77 ± 0.03	0.73 ± 0.03*	-5%	0.86 ± 0.08	0.84 ± 0.05	-2%
CORT	2.03 ± 0.31	1.65 ± 0.26*	-19%	1.13 ± 0.39	1.10 ± 0.28	-3%
PFC	0.58 ± 0.07	0.57 ± 0.04	-2%	0.76 ± 0.05	0.73 ± 0.05	-4%

Data were obtained in test cohorts 4 and 5. Results are shown as mean ± SD. WT: wild type, PKU: phenylketonuric. Δ shows the difference between mean PKU values and mean WT values, expressed as percentage change compared to mean WT values. DGi: inner layer of the dentate gyrus, DGo: outer layer of the dentate gyrus, CA: cornu ammonis, STR: striatum, CORT: somatosensory cortex, PFC: prefrontal cortex. * $p<0.05$ PKU vs corresponding WT.

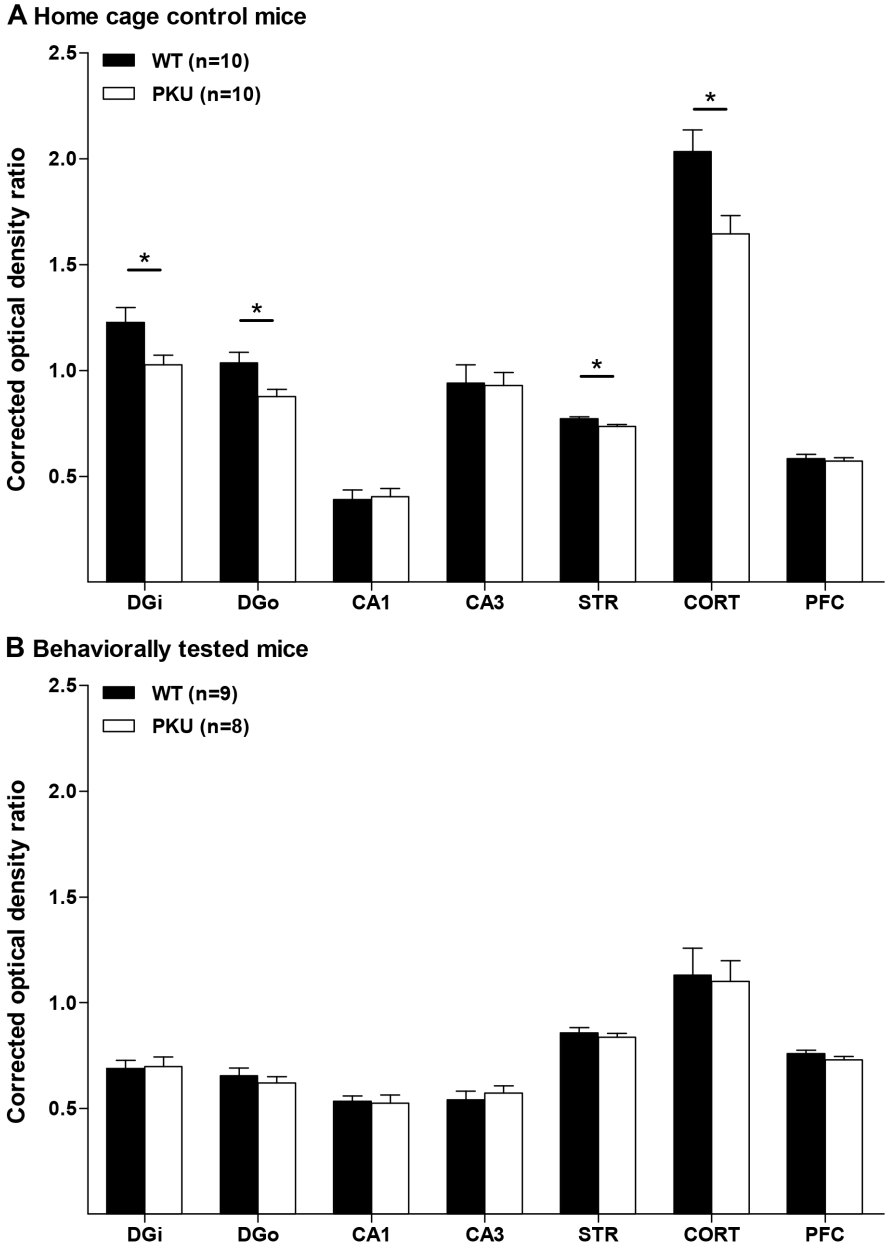

Figure 5 pCREB/CREB ratios for corrected optical density in home cage control mice (A; test cohort 4) and behaviorally tested mice (B; test cohort 5). WT: wild type. PKU: phenylketonuric. Results are shown as mean values with SEM as error bars. * $p<0.05$ PKU vs WT. DGi: inner layer of the dentate gyrus, DGo: outer layer of the dentate gyrus, CA: cornu ammonis, STR: striatum, CORT: somatosensory cortex, PFC: prefrontal cortex.

Discussion

In this study, we investigated learning and memory in relation to brain CREB phosphorylation in C57Bl/6 Pah-enu2 PKU mice. The main findings are the absence of learning and memory deficits in C57Bl/6 PKU mice, the reduced pCREB/CREB ratios in several brain regions in home cage control PKU mice, and the absence of reduced pCREB/CREB ratios in behaviorally tested PKU mice, compared to C57Bl/6 non-PKU mice.

Contrary to our hypothesis, we did not find learning and memory deficits in C57Bl/6 PKU mice. Of note, our home cage control C57Bl/6 PKU mice showed the typical biochemical characteristics of untreated PKU, i.e. markedly elevated blood Phe concentrations, elevated brain Phe concentrations, reduced brain concentrations of non-Phe LNAAs, and reduced brain concentrations of monoaminergic neurotransmitters. Other authors have reported similar biochemical results in C57Bl/6 PKU mice (39-42). In addition, the degrees of the biochemical alterations observed in the current study are comparable to those reported previously (39-42). Therefore, the absence of learning and memory deficits in our C57Bl/6 PKU mice does not appear to result from atypical biochemical phenotypes.

When interpreting the behavioral findings of this study, one may wonder to which extent these findings correspond to previously published data. For the results regarding spontaneous alternation in the Y maze, learning and reversal learning in the Y maze, novel object recognition testing, and spatial object recognition testing, performance of non-PKU control mice was comparable to previously published findings in the C57Bl/6 strain (36,45-48,55-59). In the ten-arm radial maze, a new paradigm developed by our group, PKU mice appeared to perform worse than WT mice during sessions 8, 9, 10, and 11. However, these apparent differences in performance scores did not reach statistical significance. Since, to our knowledge, this study is the first to describe the use of this particular set-up in C57Bl/6 mice, performance results of WT mice could not be compared with previously published data. In the cross maze, both WT and PKU mice showed comparable performance results during cross-maze training, mastering the task in a few sessions. The cross maze results of this study correspond well with previously published C57Bl/6 data (60-62), although performance scores at the first training session were relatively high in test cohort 5. These relatively high scores likely related to the position of the baited arm relative to the starting arm, which was similar in the cross maze task and ten-arm radial maze task. In support of this interpretation, in WT and PKU mice that had not been behaviorally tested previously (i.e. test cohort 6), performance scores on the first training session were ~50%, as in previous reports (48,62). In the cross-maze probe trials, both WT and PKU mice showed behavior consistent with

a strong preference for using a non-spatial strategy. This strategy preference differs from previous reports showing that C57Bl/6 WT mice generally prefer using a spatial strategy in this paradigm (48,61,62). Possibly, an increased number of extra-maze spatial cues would have facilitated the preference for a spatial strategy in our cross maze experiments.

In home cage control PKU mice, reduced pCREB/CREB ratios compared to home cage control WT mice were observed in the dentate gyrus, the striatum, and the somatosensory cortex. Even relatively slight reductions in CREB Ser-133 phosphorylation in the 10-20% range have been associated with learning and memory deficits (48,63-65). These data suggest that the reduced pCREB/CREB ratios as observed in our study may have functional consequences. Thus, reduced CREB Ser-133 phosphorylation could underlie the reduced CPS previously reported in PKU, in both patients and mice (1,12-15,66). Contrary to the reduced pCREB/CREB ratios in home cage control PKU mice, pCREB/CREB ratios of behaviorally tested PKU mice did not differ from those of corresponding WT mice. Thus, behavioral testing appeared to normalize the reduced pCREB/CREB ratios present in home cage control PKU mice. In this context, it should be noted that both behavioral paradigms used in relation to the calculation of pCREB/CREB ratios (i.e. the ten-arm radial maze and the cross maze) involved food restriction. Thus, it may be postulated that food restriction contributed to the apparent normalization of pCREB/CREB ratios. To our knowledge, the effects of food restriction on brain pCREB/CREB ratios in rodents have been reported for rat striatum only (67-70). In these studies, which involved a more stringent food restriction regime than our current study, pCREB/CREB ratios were unaffected by food restriction. Therefore, we consider the apparent normalization of reduced pCREB/CREB ratios in behaviorally tested PKU mice to be most likely caused by behavioral testing, rather than by food restriction. This conclusion suggests that C57Bl/6 PKU mice are able to restore CREB phosphorylation during behavioral testing by an as yet uncharacterized mechanism, and thus preserve learning and memory.

It may seem tempting to directly compare the immunohistochemical results of home cage control mice and behaviorally tested mice by genotype group. However, it should be noted that this study focused on comparing PKU and WT mice within each test cohort, rather than comparing immunohistochemical parameters across test cohorts. The immunohistochemical analyses of home cage control mice and behaviorally tested mice were performed in different sessions. Thus, the comparison between PKU mice and WT mice within each test cohort can be made reliably, whereas the comparison between home cage control mice and behaviorally tested mice should be made with caution.

When considering the upstream mechanisms underlying the reduced pCREB/CREB ratios in home cage control PKU mice, the question arises which kinases could be involved. Currently, about 15 kinases phosphorylating CREB to pCREB at Ser-133 have been reported (19,20). These kinases respond to an even wider range of possible stimuli (19,20). In relation to existing pathophysiological knowledge on PKU, several kinases appear to be particularly interesting, i.e. protein kinase A (PKA), protein kinase C (PKC), kinases belonging to the mitogen-activated protein kinase/extracellular signal-regulated kinase (MAPK/ERK) and Ca^{2+}/calmodulin-dependent protein kinase (CaMK) families, and the eukaryotic initiation factor 2α (eIF2α). These kinases regulate CREB phosphorylation at Ser-133 in response to dopaminergic, serotonergic, and glutamatergic signaling, as well as under conditions of essential amino acid deficiency. Impaired dopaminergic and serotonergic signaling may result from the reduced brain concentrations of these neurotransmitters observed in PKU. In BTBR PKU mice, impaired glutamatergic signaling and reduced CaMK phosphorylation have been reported (71-73). The final kinase mentioned above, eIF2α, reduces CREB phosphorylation at Ser-133 in response to several physiological stressors, including essential amino acid deficiency (74-76). As almost all LNAAs are essential amino acids, reduced brain concentrations of non-Phe LNAAs (as observed in our current study and elsewhere (14,29,31,40,41)) could increase eIF2α kinase activity. The aforementioned kinases may thus reduce CREB Ser-133 phosphorylation, either alone or in combination. Lastly, the reduced pCREB/CREB ratios may result from increased dephosphorylation, which could be mediated by protein phosphatase 1 and/or protein phosphatase 2 (17,19,20).

The findings of our study may have both fundamental and clinical relevance. Fundamentally, our data provide additional insight into the pathophysiology of cognitive dysfunction in PKU, combining the fields of inborn errors of metabolism and molecular neurobiology. As such, the findings of this study are not only relevant for those working in the PKU field, but also for those interested in the neurobiology of learning and memory. Clinically, the characterization of pathways critically involved in PKU pathophysiology may lead to new, mechanism-based treatments. Such treatments could reduce treatment burden and improve cognitive outcome and quality of life in PKU.

In summary, we performed a series of experiments to investigate learning and memory, LNAA and neurotransmitter concentrations, and immunoreactivity for CREB and pCREB in C57Bl/6 Pah-enu2 PKU mice. Despite the presence of biochemical profiles characteristic of PKU and despite reduced pCREB/CREB ratios in several brain regions in home cage control PKU mice, behaviorally tested C57Bl/6 PKU mice did not show learning and memory deficits. In behaviorally tested PKU

mice, pCREB/CREB ratios were comparable to those of behaviorally tested WT mice. The normalization of reduced pCREB/CREB ratios, which was likely induced by behavioral testing, appeared to preserve learning and memory in behaviorally tested C57Bl/6 PKU mice. Further research is needed to identify the processes upstream and downstream of reduced CREB phosphorylation in PKU, as well as the mechanisms involved in normalizing CREB phosphorylation and preserving learning and memory.

Acknowledgments

The authors are indebted to Dicky Struik, Jolijn Ronken, Elisabeth van der Spoel, Matthias Wubs, Jan Keijser, Folkert Postema, Bert Venema, Hermi Kingma, Fjodor van der Sluijs, Pim Modderman, Pim de Blauw, Janneke van der Molen-Kooistra, Vera Ruttgers-Brattinga, Margreet Schaaf, Enge Hoolsema, and Hillie Adema. Their assistance is kindly acknowledged.

References

1. Blau N, van Spronsen FJ, Levy HL (2010) Phenylketonuria. Lancet 376: 1417-1427.
2. van Spronsen FJ (2010) Phenylketonuria: a 21st century perspective. Nat. Rev. Endocrinol. 6: 509-514.
3. Christ SE, Huijbregts SC, de Sonneville LM, White DA (2010) Executive function in early-treated phenylketonuria: profile and underlying mechanisms. Mol. Genet. Metab. 99 Suppl 1: S22-S32.
4. Huijbregts SC, Gassio R, Campistol J (2013) executive functioning in context: Relevance for treatment and monitoring of phenylketonuria. Mol. Genet. Metab. 110 Suppl: S25-S30.
5. Smith I, Knowles J (2000) Behaviour in early treated phenylketonuria: a systematic review. Eur. J. Pediatr. 159 Suppl 2: S89-S93.
6. Surtees R, Blau N (2000) The neurochemistry of phenylketonuria. Eur. J. Pediatr. 159 Suppl 2: S109-S113.
7. de Groot MJ, Hoeksma M, Blau N, Reijngoud DJ, van Spronsen FJ (2010) Pathogenesis of cognitive dysfunction in phenylketonuria: review of hypotheses. Mol. Genet. Metab. 99 Suppl 1: S86-S89.
8. Greer PL, Greenberg ME (2008) From synapse to nucleus: calcium-dependent gene transcription in the control of synapse development and function. Neuron 59: 846-860.
9. Vaillend C, Poirier R, Laroche S (2008) Genes, plasticity and mental retardation. Behav. Brain Res. 192: 88-105.
10. Johnston MV (2003) Brain plasticity in paediatric neurology. Eur. J. Paediatr. Neurol. 7: 105-113.
11. Wall KM, Pardridge WM (1990) Decreases in brain protein synthesis elicited by moderate increases in plasma phenylalanine. Biochem. Biophys. Res. Commun. 168: 1177-1183.
12. Paans AM, Pruim J, Smit GP, Visser G, Willemsen AT, Ullrich K (1996) Neurotransmitter positron emission tomographic-studies in adults with phenylketonuria, a pilot study. Eur. J. Pediatr. 155 Suppl 1: S78-S81.
13. Pardridge WM (1998) Blood-brain barrier carrier-mediated transport and brain metabolism of amino acids. Neurochem. Res. 23: 635-644.
14. Smith CB, Kang J (2000) Cerebral protein synthesis in a genetic mouse model of phenylketonuria. Proc. Natl. Acad. Sci. U. S. A. 97: 11014-11019.
15. Hoeksma M, Reijngoud DJ, Pruim J, de Valk HW, Paans AM, van Spronsen FJ (2009) Phenylketonuria: High plasma phenylalanine decreases cerebral protein synthesis. Mol. Genet. Metab. 96: 177-182.
16. Cardin JA, Abel T (1999) Memory suppressor genes: enhancing the relationship between synaptic plasticity and memory storage. J. Neurosci. Res. 58: 10-23.
17. Josselyn SA, Nguyen PV (2005) CREB, synapses and memory disorders: past progress and future challenges. Curr. Drug Targets CNS Neurol. Disord. 4: 481-497.
18. Wu H, Zhou Y, Xiong ZQ (2007) Transducer of regulated CREB and late phase long-term synaptic potentiation. FEBS J. 274: 3218-3223.
19. Sakamoto K, Karelina K, Obrietan K (2011) CREB: a multifaceted regulator of neuronal plasticity and protection. J. Neurochem. 116: 1-9.
20. Johannessen M, Delghandi MP, Moens U (2004) What turns CREB on? Cell. Signal. 16: 1211-1227.
21. Basavarajappa BS, Subbanna S (2014) CB1 receptor-mediated signaling underlies the hippocampal synaptic, learning, and memory deficits following treatment with JWH-081, a new component of

spice/K2 preparations. Hippocampus 24: 178-188.

22. Mitsui S, Osako Y, Yokoi F, Dang MT, Yuri K, Li Y, Yamaguchi N (2009) A mental retardation gene, motopsin/neurotrypsin/prss12, modulates hippocampal function and social interaction. Eur. J. Neurosci. 30: 2368-2378.
23. Li Q, Zhao HF, Zhang ZF, et al. (2009) Long-term administration of green tea catechins prevents age-related spatial learning and memory decline in C57BL/6J mice by regulating hippocampal cyclic amp-response element binding protein signaling cascade. Neuroscience 159: 1208-1215.
24. Sakurai M, Sekiguchi M, Zushida K, Yamada K, Nagamine S, Kabuta T, Wada K (2008) Reduction in memory in passive avoidance learning, exploratory behaviour and synaptic plasticity in mice with a spontaneous deletion in the ubiquitin C-terminal hydrolase L1 gene. Eur. J. Neurosci. 27: 691-701.
25. Porte Y, Buhot MC, Mons NE (2008) Spatial memory in the Morris water maze and activation of cyclic AMP response element-binding (CREB) protein within the mouse hippocampus. Learn. Mem. 15: 885-894.
26. Shedlovsky A, McDonald JD, Symula D, Dove WF (1993) Mouse models of human phenylketonuria. Genetics 134: 1205-1210.
27. Martynyuk AE, van Spronsen FJ, van der Zee EA (2010) Animal models of brain dysfunction in phenylketonuria. Mol. Genet. Metab. 99 Suppl 1: S100-S105.
28. Zagreda L, Goodman J, Druin DP, McDonald D, Diamond A (1999) Cognitive deficits in a genetic mouse model of the most common biochemical cause of human mental retardation. J. Neurosci. 19: 6175-6182.
29. Pascucci T, Ventura R, Puglisi-Allegra S, Cabib S (2002) Deficits in brain serotonin synthesis in a genetic mouse model of phenylketonuria. Neuroreport 13: 2561-2564.
30. Cabib S, Pascucci T, Ventura R, Romano V, Puglisi-Allegra S (2003) The behavioral profile of severe mental retardation in a genetic mouse model of phenylketonuria. Behav. Genet. 33: 301-310.
31. Pascucci T, Andolina D, Ventura R, Puglisi-Allegra S, Cabib S (2008) Reduced availability of brain amines during critical phases of postnatal development in a genetic mouse model of cognitive delay. Brain Res. 1217: 232-238.
32. Ding Z, Georgiev P, Thony B (2006) Administration-route and gender-independent long-term therapeutic correction of phenylketonuria (PKU) in a mouse model by recombinant adeno-associated virus 8 pseudotyped vector-mediated gene transfer. Gene Ther. 13: 587-593.
33. Crawley JN, Belknap JK, Collins A, et al. (1997) Behavioral phenotypes of inbred mouse strains: implications and recommendations for molecular studies. Psychopharmacology (Berl) 132: 107-124.
34. Holmes A, Wrenn CC, Harris AP, Thayer KE, Crawley JN (2002) Behavioral profiles of inbred strains on novel olfactory, spatial and emotional tests for reference memory in mice. Genes Brain Behav. 1: 55-69.
35. Mishina M, Sakimura K (2007) Conditional gene targeting on the pure C57BL/6 genetic background. Neurosci. Res. 58: 105-112.
36. Molenhuis RT, de Visser L, Bruining H, Kas MJ (2014) Enhancing the value of psychiatric mouse models; differential expression of developmental behavioral and cognitive profiles in four inbred strains of mice. Eur. Neuropsychopharmacol. 24: doi: 10.1016/j.euroneuro.2014.01.013.
37. Watase K, Zoghbi HY (2003) Modelling brain diseases in mice: the challenges of design and analysis. Nat. Rev. Genet. 4: 296-307.

38. Welzl H, D'Adamo P, Wolfer DP, Lipp HP (2006) In: Transgenic and knockout models of neuropsychiatric disorders. Mouse models of hereditary mental retardation. Fisch GS, Flint J, eds. Totowa, NJ: Humana Press, 101-125.

39. Arning E, Bottiglieri T, Sun Q, et al. (2009) Metabolic profiling in phenylalanine hydroxylase deficient (Pah-/-) mouse brain reveals decreased amino acid neurotransmitters and preferential alterations of the serotoninergic system. Mol. Genet. Metab. 98: 21.

40. Vogel KR, Arning E, Wasek BL, Bottiglieri T, Gibson KM (2013) Non-physiological amino acid (NPAA) therapy targeting brain phenylalanine reduction: pilot studies in Pah-enu2 mice. J. Inherit. Metab. Dis. 36: 513-523.

41. Vogel KR, Arning E, Wasek BL, Bottiglieri T, Gibson KM (2013) Characterization of 2-(methylamino) alkanoic acid capacity to restrict blood-brain phenylalanine transport in Pah-enu2 mice: preliminary findings. Mol. Genet. Metab. 110 Suppl: S71-S78.

42. Sawin EA, Murali SG, Ney DM (2014) Differential effects of low-phenylalanine protein sources on brain neurotransmitters and behavior in C57Bl/6 Pah-enu2 mice. Mol. Genet. Metab. 111: doi: 10.1016/j.ymgme.2014.01.015.

43. Lalonde R (2002) The neurobiological basis of spontaneous alternation. Neurosci. Biobehav. Rev. 26: 91-104.

44. Hughes RN (2004) The value of spontaneous alternation behavior (SAB) as a test of retention in pharmacological investigations of memory. Neurosci. Biobehav. Rev. 28: 497-505.

45. Havekes R, Nijholt IM, Luiten PG, van der Zee EA (2006) Differential involvement of hippocampal calcineurin during learning and reversal learning in a Y-maze task. Learn. Mem. 13: 753-759.

46. Havekes R, Timmer M, van der Zee EA (2007) Regional differences in hippocampal PKA immunoreactivity after training and reversal training in a spatial Y-maze task. Hippocampus 17: 338-348.

47. van der Borght K, Havekes R, Bos T, Eggen BJ, van der Zee EA (2007) Exercise improves memory acquisition and retrieval in the Y-maze task: relationship with hippocampal neurogenesis. Behav. Neurosci. 121: 324-334.

48. Hagewoud R, Havekes R, Tiba PA, et al. (2010) Coping with sleep deprivation: shifts in regional brain activity and learning strategy. Sleep 33: 1465-1473.

49. Aimone JB, Deng W, Gage FH (2011) Resolving new memories: a critical look at the dentate gyrus, adult neurogenesis, and pattern separation. Neuron 70: 589-596.

50. Sahay A, Wilson DA, Hen R (2011) Pattern separation: a common function for new neurons in hippocampus and olfactory bulb. Neuron 70: 582-588.

51. Schmidt B, Marrone DF, Markus EJ (2012) Disambiguating the similar: the dentate gyrus and pattern separation. Behav. Brain Res. 226: 56-65.

52. Gold PE (2004) Coordination of multiple memory systems. Neurobiol. Learn. Mem. 82: 230-242.

53. van der Meer M, Kurth-Nelson Z, Redish AD (2012) Information processing in decision-making systems. Neuroscientist 18: 342-359.

54. Colombo PJ, Brightwell JJ, Countryman RA (2003) Cognitive strategy-specific increases in phosphorylated cAMP response element-binding protein and c-Fos in the hippocampus and dorsal striatum. J. Neurosci. 23: 3547-3554.

55. Pothion S, Bizot JC, Trovero F, Belzung C (2004) Strain differences in sucrose preference and in the

consequences of unpredictable chronic mild stress. Behav. Brain Res. 155: 135-146.

56. Mandillo S, Tucci V, Holter SM, et al. (2008) Reliability, robustness, and reproducibility in mouse behavioral phenotyping: a cross-laboratory study. Physiol. Genomics 34: 243-255.

57. Catania EH, Pimenta A, Levitt P (2008) Genetic deletion of Lsamp causes exaggerated behavioral activation in novel environments. Behav. Brain Res. 188: 380-390.

58. Goodman T, Trouche S, Massou I, Verret L, Zerwas M, Roullet P, Rampon C (2010) Young hippocampal neurons are critical for recent and remote spatial memory in adult mice. Neuroscience 171: 769-778.

59. Boulware MI, Heisler JD, Frick KM (2013) The memory-enhancing effects of hippocampal estrogen receptor activation involve metabotropic glutamate receptor signaling. J. Neurosci. 33: 15184-15194.

60. Hagewoud R, Havekes R, Tiba PA, et al. (2010) Coping with sleep deprivation: shifts in regional brain activity and learning strategy. Sleep 33: 1465-1473.

61. Passino E, Middei S, Restivo L, Bertaina-Anglade V, Ammassari-Teule M (2002) Genetic approach to variability of memory systems: analysis of place vs. response learning and fos-related expression in hippocampal and striatal areas of C57BL/6 and DBA/2 mice. Hippocampus 12: 63-75.

62. Middei S, Restivo L, Sgobio C, Passino E, Ammassari-Teule M (2004) Reversible inactivation of hippocampus and dorsolateral striatum in C57BL/6 and DBA/2 inbred mice failed to show interaction between memory systems in these genotypes. Behav. Brain Res. 154: 527-534.

63. Hagewoud R, Bultsma LJ, Barf RP, Koolhaas JM, Meerlo P (2011) Sleep deprivation impairs contextual fear conditioning and attenuates subsequent behavioural, endocrine and neuronal responses. J. Sleep Res. 20: 259-266.

64. Morice E, Farley S, Poirier R, et al. (2013) Defective synaptic transmission and structure in the dentate gyrus and selective fear memory impairment in the Rsk2 mutant mouse model of Coffin-Lowry syndrome. Neurobiol. Dis. 58: 156-168.

65. Palmeri A, Privitera L, Giunta S, Loreto C, Puzzo D (2013) Inhibition of phosphodiesterase-5 rescues age-related impairment of synaptic plasticity and memory. Behav. Brain Res. 240: 11-20.

66. de Groot MJ, Hoeksma M, Reijngoud DJ, de Valk HW, Paans AM, Sauer PJ, van Spronsen FJ (2013) Phenylketonuria: reduced tyrosine brain influx relates to reduced cerebral protein synthesis. Orphanet J. Rare Dis. 8: 133-141.

67. Haberny SL, Berman Y, Meller E, Carr KD (2004) Chronic food restriction increases D-1 dopamine receptor agonist-induced phosphorylation of extracellular signal-regulated kinase 1/2 and cyclic AMP response element-binding protein in caudate-putamen and nucleus accumbens. Neuroscience 125: 289-298.

68. Pan Y, Berman Y, Carr KD (2004) Effects of the group I metabotropic glutamate receptor agonist, DHPG, and injection stress on striatal cell signaling in food-restricted and ad libitum fed rats. BMC Neurosci. 5: 50.

69. Haberny SL, Carr KD (2005) Food restriction increases NMDA receptor-mediated calcium-calmodulin kinase II and NMDA receptor/extracellular signal-regulated kinase 1/2-mediated cyclic AMP response element-binding protein phosphorylation in nucleus accumbens upon D-1 dopamine receptor stimulation in rats. Neuroscience 132: 1035-1043.

70. Cabeza de Vaca S, Kannan P, Pan Y, Jiang N, Sun Y, Carr KD (2007) The adenosine A2A receptor agonist, CGS-21680, blocks excessive rearing, acquisition of wheel running, and increases nucleus

accumbens CREB phosphorylation in chronically food-restricted rats. Brain Res. 1142: 100-109.

71. Glushakov AV, Dennis DM, Morey TE, Sumners C, Cucchiara RF, Seubert CN, Martynyuk AE (2002) Specific inhibition of N-methyl-D-aspartate receptor function in rat hippocampal neurons by L-phenylalanine at concentrations observed during phenylketonuria. Mol. Psychiatry 7: 359-367.
72. Glushakov AV, Dennis DM, Sumners C, Seubert CN, Martynyuk AE (2003) L-phenylalanine selectively depresses currents at glutamatergic excitatory synapses. J. Neurosci. Res. 72: 116-124.
73. Glushakov AV, Glushakova O, Varshney M, et al. (2005) Long-term changes in glutamatergic synaptic transmission in phenylketonuria. Brain 128: 300-307.
74. Zhang P, McGrath BC, Reinert J, et al. (2002) The GCN2 eIF2alpha kinase is required for adaptation to amino acid deprivation in mice. Mol. Cell. Biol. 22: 6681-6688.
75. Wek RC, Jiang HY, Anthony TG (2006) Coping with stress: eIF2 kinases and translational control. Biochem. Soc. Trans. 34: 7-11.
76. Costa-Mattioli M, Sossin WS, Klann E, Sonenberg N (2009) Translational control of long-lasting synaptic plasticity and memory. Neuron 61: 10-26.